DOI: 10.1002/anie.201004794

Oxygen Reduction

Theoretical Studies of Potential-Dependent and Competing Mechanisms of the Electrocatalytic Oxygen Reduction Reaction on Pt(111)**

*John A. Keith and Timo Jacob**

The oxygen reduction reaction (ORR) is a key process in combustion, corrosion, cellular respiration, and energy technology. Under electrochemical conditions with a supply of hydrogen, the electrocatalytic ORR[1] is also the reaction that allows polymer-electrolyte (or proton-exchange) membrane fuel cells (PEMFCs) to operate. Economic and environmental factors are driving research to develop practical and environmentally sustainable energy sources as well as long-living heterogeneous catalysts. The ORR is expected to play a central role in these technologies, but a more fundamental understanding of the ORR is needed.

An atomic-level understanding of the ORR mechanism is still in its early stages because of the high complexity of ORR kinetics. What is known, however, is that the complete electrochemical ORR involves four net coupled proton and electron transfers (CPETs) to molecular oxygen at the cathode. Although the idealized electrochemical reaction generates 1.23 V per electron (Scheme 1), the standard operating potential for the electrocatalytic ORR on Pt(111) is below 0.9 V. Determining the cause of this overpotential of about 0.3 V and improving the overall activity (increasing the current density) are the keys to improving ORR catalyst design and to better harness the ORR as a practical means for energy conversion. Some ORR processes are believed to lead to surface oxides and/or strongly binding intermediates, which in turn are expected as hindrances of the ORR.[1] Thus, designing new heterogeneous catalysts that destabilize these intermediates without changing the overall mechanism is desired.

$$2\,H_{2(g)} \rightarrow 4\,H^{+}_{(aq)} + 4\,e^{-} \qquad E^{\circ} = 0\,V$$

$$O_{2(g)} + 4\,H^{+}_{(aq)} + 4\,e^{-} \rightarrow 2\,H_2O_{(l)} \qquad E^{\circ} = 1.229\,V$$

$$\text{Total: } 2\,H_{2(g)} + O_{2(g)} \rightarrow 2\,H_2O_{(l)} \qquad U = 1.229\,V$$

Scheme 1. Hydrogen oxidation (at the anode) and oxygen reduction reactions (at the cathode) at fuel-cell electrodes.

Whilst possible ORR intermediates only consist of H and O atoms, the ORR mechanism is elusive, even on the highly studied Pt(111) electrodes. There have been substantial efforts over the past decade to use first-principles quantum mechanics (QM) calculations to determine binding energies (BEs) of oxygen on platinum and other transition metal surfaces and to extend those data to investigate aspects of the ORR mechanism,[2] and even investigate the role of an applied electrode potential on a reaction mechanism.[3] Most relevantly, QM calculations can provide accurate descriptions of chemical bonding energies, which can be used to predict ORR rate constants. Calculating these values is a first step towards understanding the complete electrocatalytic ORR from first principles, something that will likely require a multiscale analysis explicitly addressing the electrochemical double layer, electron dynamics, surface-coverage effects, and transport issues. Although such a complete simulation is not yet feasible, energies and barriers based on QM calculations can be used in a kinetic model and then compared to experimental observables. If the rate constants obtained from first-principles calculations rationalized features of the ORR, this would be a large step towards fundamentally understanding this and other highly complex reactions.

Constructing a physically reasonable heterogeneous ORR mechanism requires explicitly determining the BEs of a list of possible intermediates: O*, H*, O_2*, OH*, OOH*, H_2O_2*, and H_2O* as well as the transition states that link the intermediates to one another. For generality, we consider that electrochemical reactions may operate by Langmuir–Hinshelwood (LH) or Eley–Rideal (ER) mechanisms. LH mechanisms involve all the reacting intermediates on the surface, whereas ER mechanisms involve species from the electrolyte reacting with a surface intermediate (for example H_3O^+). Characterization of key steps on the idealized Pt(111) surface allows analogous steps on imperfect or modified surfaces to also be calculated and then compared to experiment.

Developing a reliable calculation model for such a study is especially arduous.[4] Herein, we used a Pt_{35} cluster as a basis for first-principles density functional theory (DFT) calculations on the electrocatalytic ORR on Pt(111). Calculations were run at the B3LYP/LACVP** level as calculated by the Jaguar program.[5] Unlike most other cluster models, this model is relatively large and contains three-layers of atoms fixed to experimental bulk distances with four atoms relaxed at the Pt(111) surface. Although substantially smaller clusters have been used to model catalytic reactions such as the ORR, in extensive cluster-size convergence studies we found that a

[*] Dr. J. A. Keith, Dr. T. Jacob
Institut für Elektrochemie, Universität Ulm
Albert-Einstein-Allee 47, 89081 Ulm (Germany)
Fax: (+49) 731-502-5409
E-mail: timo.jacob@uni-ulm.de
Homepage: http://www.echem.uni-ulm.de

[**] We gratefully acknowledge financial support from the Alexander von Humboldt foundation, the Deutsche Forschungsgemeinschaft (DFG) within the Emmy Noether program, and the EU network ELCAT (Proposal No. 214936-2, 2008-2012). We also thank Prof. Dr. D. M. Kolb and Dr. L. A. Kibler for helpful discussions.

three-layered Pt_{28} cluster is the smallest and shallowest cluster capable of giving converged BEs.[4a] The present study is based on calculations on a slightly larger Pt_{35} cluster, which was found to accurately model the extended Pt(111) surface and its behavior in catalytic reactions.[4b,c] We report stable surface sites and BEs on Pt(111) for each ORR intermediate whilst confirming convergence of spin, energy, and geometry for each intermediate. By doing so, our BE calculations agree quite well with periodic slab calculations.

Computational convergence alone is not enough to show a model is capable of reliable mechanistic predictions, so we confirmed our calculations alongside available experimental values. We tested the approach by comparing our calculated gas phase energies against those obtained from low-temperature and low-pressure surface experiments. Thermal desorption spectroscopy (TDS)[6] and electron energy-loss spectroscopy (EELS)[7] have determined the low-coverage BEs of O_2* to be 0.3–0.5 eV, O* to be 3.47–3.73 eV (referenced to atomic oxygen), and H_2O* to be 0.43–0.65 eV.[8] The dissociation barrier for O_2*→2 O* on Pt(111) is estimated to be the same as the BE of O_2* based on these experiments. Scanning tunneling microscopy (STM) measurements[9] have also shown that whilst O_2* prefers to bind at a bridge site, its molecular dissociation occurs via a different O_2* intermediate on Pt(111).

Our calculations reproduce these observations with respectable accuracy. The calculated BEs for O_2*, O*, and H_2O* were 0.49 eV, 3.25 eV, and 0.60 eV, respectively. Additionally, the calculated O*–O* dissociation barrier was overall 0.65 eV and involved O_2* bound at an fcc site. To simulate electrochemical conditions, we calculated electronic energies [E_{SCF}; Equation (1)], vibrational zero-point energies (E_{ZPE}), vibrational components of thermodynamic partition functions from the ideal gas approximation ($S_{vib}(T)$ and $H_{vib}(T)$), and single-point solvation energies in water calculated with the Jaguar[5] Poisson–Boltzmann solver (E_{SCRF}), all from first principles [Eq. (2)]. More details of how these energy values vary for different reaction intermediates can be found in Ref. [4cd]. Unfortunately, direct comparison to experimental observations arising from these individual energy terms is not possible as electrochemical ORR experiments focus on overall activity rather than individual BEs.

Gas phase $\quad \Delta E_{gas} = \Delta E_{SCF}$ (1)

Free energy

$$\Delta G_{solv,T} = \Delta E_{SCF} + \Delta E_{SCRF} + \Delta E_{ZPE} + \Delta H_{vib}(T) - T\,\Delta S_{vib}(T) \quad (2)$$

A significant challenge arises in comparing calculations to electrocatalytic ORR experiments owing to disagreement over interpretations of certain experiments. There is agreement that the first electron-transfer process in the ORR is rate-determining over a wide potential range. There is however disagreement about the nature of this first electron transfer. Damjanovic et al. first proposed the proton-coupled process $O_2* + H^+ + e^- \rightarrow HO_2*$,[10] whereas Yeager et al. proposed rate-determining reductive and dissociative adsorption of O_2*→2 O* (catalyzed by an electron transfer) as being rate-determining.[11] The observation of a single Tafel slope for a large potential region argues in favor of Damjanovic's proposal,[12] though the proton-less process, $O_2* + e^- \rightarrow O_2*^-$, is now often used as a central feature in general electrocatalytic ORR analyses, and not just for ORR reactions in alkaline solutions.

The strong electronic coupling between an adsorbate such as O_2* and the metal surface means a certain partial charge will flow from the charge reservoir (here the Pt electrode) to more electronegative atoms (such as O) upon adsorption. This would not occur as discrete one-electron transfer, though under some circumstances it could appear as one. Indeed, recent electronic structure calculations by Li and co-workers indicate that the perception of ionic intermediates with integer charges on surfaces is not valid on an atomic scale.[13] Subsequently, using empirical models to study an explicit charge transfer to a surface adsorbate is likely not a physically grounded route to understanding the ORR.

For this first-principles investigation, we use the general proposal from Damjanovic and Brusic,[10a] and assume electron transfers are coupled with a proton transfer as well. Therefore, we treat each one-electron reduction as an overall CPET process. This assumption permits us to use a common approach of treating an applied potential by explicitly shifting the Fermi level of the electrode (see Ref. [14] for more details). Energies for intermediates undergoing a net CPET will be shifted by $+eU$, where e is the elementary charge and U is the electrode potential (referenced to the reversible hydrogen electrode; RHE) applied within the calculation. Regarding the proton transfers to the surface, we have used a multistep procedure based first-principles data, which has been described in detail in Ref. [4d].

In our previous study,[4c] we used non-electrochemical LH-type reactions (that is, where all reacting intermediates reside on the surface), and reported our calculations without the influence of an electrode potential. Herein we present a full mechanistic study, including potential-dependent ER and LH mechanisms. CPET processes occurring either by an LH or an ER mechanism are labeled in Scheme 2 with an asterisk. Potential-dependent LH mechanisms are calculated as before, with the exception that H* species arise from CPET reactions from aqueous H^+. Thus, each inclusion of H* is accompanied by an electron transfer, leading to a shift in the intermediate energy by $+eU$. We present results from the reaction pathways shown in Scheme 2 using potential-depen-

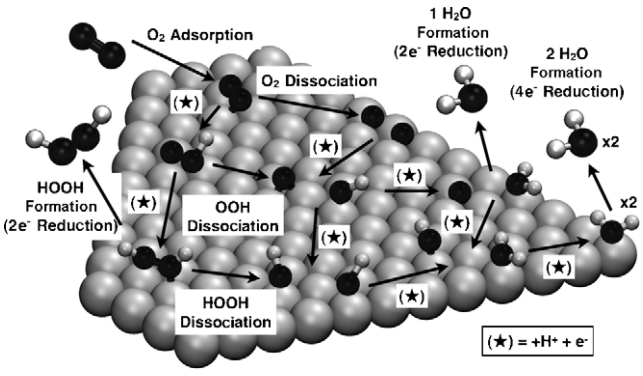

Scheme 2. Possible reaction mechanisms of the ORR on Pt(111).

dent ΔG energies calculated at 298 K [Eq. (2)]. We consider three possible mechanisms that are based on adsorbed intermediates:

1. The O_2 pathway: Adsorption of O_2 is followed by dissociation into 2 O*. The O* intermediates then undergo four CPETs, leading to two water molecules (in the four-electron pathway). Owing to strongly adsorbed O* species, the O_2 dissociation would appear in mechanisms as a one-electron reductive process.[4c]
2. The OOH pathway: Adsorption of O_2 is followed by one CPET and then O*–OH* dissociation to form O* and OH*. These intermediates may then undergo three CPETs to form two water molecules, as was the case in the O_2 pathway.
3. The HOOH pathway: Adsorption of O_2 is followed by two CPETs to form H_2O_2*. When H_2O_2* is released from the surface, this is a two-electron pathway. When H_2O_2* is allowed to dissociate on the surface, the two OH* intermediates can then undergo two CPETs to form two water molecules via a four-electron pathway.

Results at zero potential ($U = 0$ V vs. the RHE) are summarized in Figure 1 a. ΔG_{298} values of O_2*, OOH*, and HOOH* are −1.35, −1.77, and −2.03 eV, respectively. Dissociation barriers for each of these adsorbates O*–O*, O*–OH*, and HO*–OH* are 0.68, 0.59, and 0.31 eV, respectively, with barriers decreasing corresponding to the number of H atoms bound to O_2*. After these dissociations, multiple processes may lead to either 2 O*, O* + OH*, 2 OH*, or OH* + H_2O*. ΔG_{298} values for each set of adsorbates also decreases corresponding to the number of H atoms on the O* intermediates: −3.06, −3.80, −4.54, and −4.93 eV. The most strongly bound intermediate at $U = 0$ V is $2H_2O$*, with a BE of 0.75 eV with respect to $2H_2O_{(l)}$ (or a relative free energy of −5.33 eV with respect to $H_{2(g)} + O_{2(g)}$). The entire ORR process denoted in Scheme 1 is 4.57 eV exothermic in energy at $U = 0$ V.

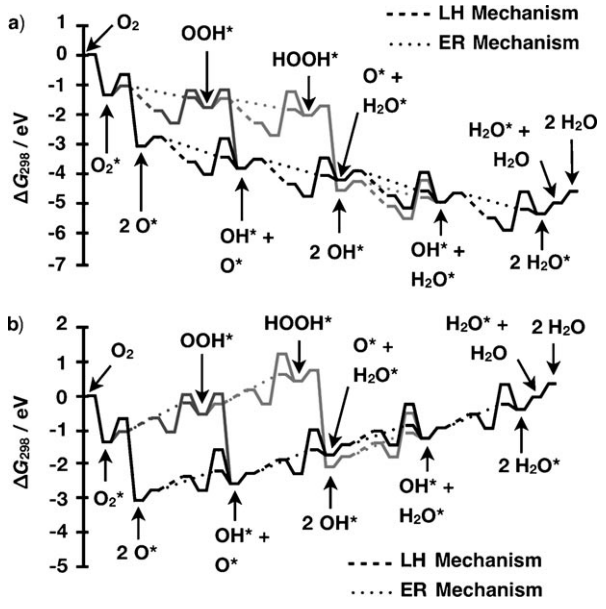

Figure 1. Reaction energies (relative to molecular $O_2 + 2H_2$) for ORR pathways according to Scheme 2. Energies in (a) correspond to calculations at no applied potential, whereas results in (b) correspond to an applied potential of 1.23 V (vs. RHE). Dashed and dotted lines denote CPET processes through the double layer.[4d]

Although trends are clearly seen from these energies, LH-type reaction barriers are more complicated. LH barriers leading to OH*, H_2O*, OOH*, and HOOH* are quite high: 1.19, 1.28, 1.09, and 1.46 eV, respectively. These differ from (de)protonation steps encountered in ER reactions at $U =$ 0 V, which are all approximated to be about 0.3 eV.[4d] Thus, we expect ER mechanisms to dominate over LH mechanisms at low electrode potentials.

Based on these calculations alone, one would deduce that at low potentials, ER-type mechanisms primarily operating through the HOOH pathway, as this process has the lowest energy barriers. Interestingly, the H_2O_2* intermediate cannot be characterized with periodic DFT calculations on a clean Pt(111) surface.[2a] Our own periodic DFT calculations on (3 × 3) unit cells indicate its dissociation barrier is negligibly low, however this indicates that the presence of other co-adsorbates, such as H atoms, possibly due to underpotential deposition, may prevent HO–OH bond breaking and thereby stabilizes H_2O_2* intermediates.[15]

A substantially different picture of the reaction profiles is seen when applying the ideal electrode potential of 1.23 V (that is, the Nernst potential of the ORR). Here, energy levels are shifted for each net CPET step, and the total reaction is no longer highly exothermic, but essentially thermodynamically neutral. The overall energies of O_2* remains unchanged, although the adsorbates OOH* and HOOH* are destabilized to $\Delta G_{298} = -0.54$ and + 0.43 eV. The positive ΔG_{298} value for H_2O_2* alone suggests the HOOH pathway would be shut off entirely at higher potentials. The overall ΔG_{298} value for 2 O* remains unchanged, and the ΔG_{298} values for the adsorbates O* + OH*, 2 OH*, and OH* + H_2O* are now −2.57, −2.08, and −1.24 eV. It should be noted that these energies now increase based on the number of H atoms bound to O*.

Under the influence of an electrode potential, the individual hydrogenation barriers for LH-type mechanisms as well as O*–O*, O*–OH*, and HO*–OH* dissociations remain unchanged. An increased electrode potential, however, increases ER reaction barriers significantly. The ER reaction barriers for O_2*–H, HOO*–H, O*–H, and HO*–H are each no longer about 0.3 eV as they were at $U = 0$ V, but rather 1.15, 1.16, 0.87, and 0.99 eV at $U = 1.23$ V. The quite high barriers in the first two cases support a prediction that the OOH and HOOH pathways are less favorable than the O_2 pathway at high electrode potentials. Furthermore, the increased reaction barriers at higher electrode potentials indicate that both ER- and LH-type reactions may even be in play at certain ambient conditions.

Deriving electrode currents from first principles would require a rigorous kinetics analysis incorporating various double-layer effects, such as intermediate concentrations, surface coverages, or the potential drop within the interface. While future work will address this issue, we present a simplified model that is meant to reproduce qualitative conclusions that could be found by a rigorous kinetics analysis. Rather than assume a simple linear potential

dependence across the double layer and use the standard Butler–Volmer equation to report current densities, we use Eyring's canonical transition state theory[16] and assume that the potential dependent rate constant, $k(U)$, associated for a given process is:

$$k(U) = \frac{k_B T}{h} \exp\left(\frac{-\Delta^{\ddagger} G_T(U)}{k_B T}\right) \quad (3)$$

where k_B is Boltzmann's constant, T is temperature, h is Planck's constant, and $\Delta G_T(U)$ is the potential-dependent barrier for that process, assuming that the CPET reaction is a multistep process consisting of many individual hydrogen transfers through the double layer, starting from the bulk electrolyte and ending at the electrode. In a physically rigorous double-layer model, all hydrogen-transfer barriers would be modeled dynamically[17] as well as being potential-dependent, but for simplicity, the potential dependence here only alters relative energies between the initial and final states in each CPET mechanism. Ref. [4d] provides more details on this approach.

If each intermediate is approximated as having a steady-state concentration of unity, the slowest process for each mechanism in Scheme 2 is the process with the smallest calculated rate constant for that mechanism. For clarity, we construct four different pathways, three corresponding to ingoing mechanisms ending with O*–O* (k_{O_2}), O*–OH* (k_{OOH}), and HO*–OH* (k_{HOOH}) dissociations as well as two outgoing mechanisms: that starting from O* and/or OH* leading to H_2O* (k_{out}), and that where H_2O_2 desorbs from the Pt(111) electrode ($k_{HOOH,\,off}$). Calculated potential dependent rate constants are presented in Figure 2.

Based on Figure 2 we now make general predictions about the electrocatalytic ORR mechanisms. At potentials of less than 0.4 V, H_2O_2 can easily form, and the bottlenecks for the ingoing HOOH mechanisms are either HO–OH bond dissociation (shown by k_{HOOH}), or H_2O_2 desorption from the electrode surface (shown by $k_{H_2O_2,off}$), both of which are potential independent processes in this model. Both processes are substantially faster than the bottleneck processes in the OOH mechanism (O–OH dissociation) and the O_2 mechanism (O–O dissociation). Both HOOH processes are faster than the slowest step of the H_2O formation mechanism (shown by k_{out}): removal of H_2O* from the surface.

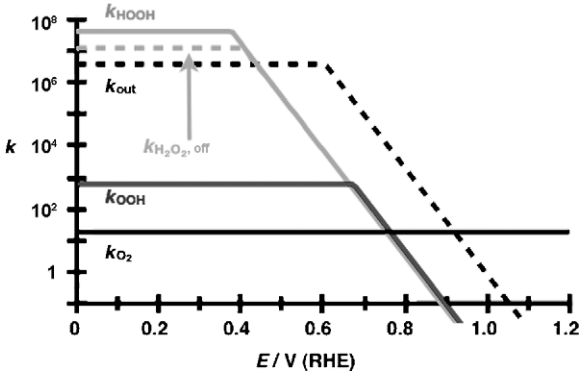

Figure 2. Potential-dependent rate constants corresponding to different ORR mechanisms. Rate constants k_{O_2}, k_{OOH}, and k_{HOOH} correspond to the smallest calculated rate constant for each mechanism ending with O*–O*, O*–OH*, and HO*–OH* dissociations, respectively. The rate constant k_{out} corresponds to the smallest calculated rate constant to create H_2O from O* and/or OH* intermediates. $k_{H_2O_2,off}$ corresponds to the rate constant for desorbing H_2O_2* from the Pt(111) electrode. The vertical axis is a measure of the relative magnitude of the rate constants. Solid lines represent ingoing mechanisms for species that adsorb onto the surface; dashed lines correspond to mechanisms that lead to the removal of surface-adsorbed species.

That k_{HOOH} is larger than k_{out} means that the bottleneck for the four-electron reduction process is in the H_2O formation steps, so intermediates such as OH* or H_2O* should be expected to accumulate on the electrode and gradually poison ORR activity. That $k_{H_2O_2,off}$ is larger than k_{out} also means that there should be a distinct probability that H_2O_2 will be released into the electrolyte showing the presence of two-electron reduction processes. Indeed, both predictions can already be confirmed with experiment. In the former case, rotating-disk experiments under acidic conditions in this potential range indicate lower ORR activity than at higher potentials.[18] For the latter, both two- and four-electron reduction processes are observed at potentials between 0.0 and 0.3 V.[1b]

At potentials of more than 0.4 V, H_2O_2 formation, a potential dependent process, becomes the bottleneck step in the HOOH mechanism, and both HOOH pathways begin to merge. Based on calculations alone, we cannot readily distinguish if the process is governed by OOH* or H_2O_2* formation, as both processes in our model have nearly identical barriers. However, that rate determining OOH* formation would be consistent with the expectation that the first electron transfer is rate-determining. As potentials increase to above 0.4 V, the H_2O_2 formation slows down owing to the potential dependence on both OOH* and H_2O_2* formation. At 0.43 V, $H_2O_{(l)}$ formation from H_2O* desorption becomes faster than any of the ingoing pathways. Although rate-determining H_2O_2 formation becomes gradually slower with increased potential, all three pathways can now be considered to contribute to the ORR activity. Furthermore, as H_2O* desorption becomes fast, surface intermediates from the ingoing mechanisms should more quickly form $H_2O_{(l)}$, and more surface sites should become available for catalysis.

At potentials above 0.6 V, H_2O formation becomes governed by potential-dependent H_2O* formation from OH*, so its rate also begins to decrease at increased potentials. At potentials of more than 0.65 V, the H_2O_2* formation mechanism has decreased to such a degree that the OOH mechanism becomes preferred. This is at nearly the same potential when potential-dependent OOH* formation from O_2* becomes the bottleneck in the OOH mechanism, and it too begins to slow down with increasing potential. At about 0.75 V, all three ingoing mechanisms have the same calculated rate constant, and at potentials of more than 0.75 V, the potential-independent O_2 mechanism becomes the preferred pathway for the potential range above 0.75 V.

At 0.95 V, H_2O* formation from OH* has slowed down to such a degree that it returns to its role as the overall bottleneck step as it was at potentials below 0.4 V. Therefore, the electrode surface will likely be saturated with O* or OH*

intermediates, causing vacant sites on the electrode to become filled and thereby stopping ORR activity. Indeed, it may be no coincidence that electrocatalytic ORR activity completely stops at about 0.9 V. We are currently implementing these calculated values into a first-principles-based kinetic model to determine the impact of surface blocking and transport diffusion to the overall ORR currents.

In conclusion, we have reported results on the first complete first-principles-based mechanistic study of the electrochemical ORR mechanism on Pt(111) electrodes. After benchmarking our QM calculations to experimental data, we report a multi-pathway electrochemical ORR mechanism that is sensitive to reaction conditions, and specifically to the applied electrode potential. A simple analysis based on calculated rate constants remarkably reproduces experimentally known factors concerning the electrocatalytic ORR, indicating the controversial atomic-scale mechanism for the ORR is becoming clearer. Future studies on the complete kinetics of these ORR pathways will be undertaken to better understand the concentration dependencies of the ORR mechanism under varied reaction conditions.

Received: August 2, 2010
Revised: September 6, 2010
Published online: October 29, 2010

Keywords: density functional calculations · electrocatalysis · heterogeneous catalysis · oxygen reduction reaction · platinum

[1] a) R. Adzic in *Electrocatalysis* (Eds.: J. Lipkowski, P. Ross, Jr.), Wiley-VCH, New York, **1998**, pp. 197–242; b) N. Marković, P. Ross, Jr. in *Interfacial Electrochemistry: Theory, Experiments and Applications* (Ed.: A. Wieckowski), Marcel Dekker, New York, **1999**, pp. 821–841; c) N. M. Marković, T. J. Schmidt, V. Stamenković, P. N. Ross, *Fuel Cells* **2001**, *1*, 105–116; d) P. Ross, Jr. in *Handbook of Fuel Cells: Fundamentals, Technology, Applications* (Eds.: W. Vielstich, A. Lamm, H. A. Gasteiger), Wiley-VCH, Weinheim, **2003**, pp. 465–480.

[2] a) A. Panchenko, M. T. M. Koper, T. E. Shubina, S. J. Mitchell, E. Roduner, *J. Electrochem. Soc.* **2004**, *151*, A2016–A2027; b) A. Eichler, F. Mittendorfer, J. Hafner, *Phys. Rev. B* **2000**, *62*, 4744–4755; c) R. A. Sidik, A. B. Anderson, *J. Electroanal. Chem.* **2002**, *528*, 69–76; d) Ž. Šljivančanin, B. Hammer, *Surf. Sci.* **2002**, *515*, 235–244; e) M. P. Hyman, J. W. Medlin, *J. Phys. Chem. B* **2006**, *110*, 15338–15344; f) R. B. Getman, W. F. Schneider, A. D. Smeltz, W. N. Delgass, F. H. Ribeiro, *Phys. Rev. Lett.* **2009**, *102*, 076101; g) Y. Sha, T. H. Yu, Y. Liu, B. V. Merinov, W. A. Goddard, *J. Phys. Chem. Lett.* **2010**, *1*, 856–861; h) L. Qi, J. Yu, J. Li, *J. Chem. Phys.* **2006**, *125*, 054701.

[3] a) A. B. Anderson, T. V. Albu, *J. Electrochem. Soc.* **2000**, *147*, 4229–4238; b) J. K. Nørskov, J. Rossmeisl, A. Logadottir, L. Lindqvist, J. R. Kitchin, T. Bligaard, H. Jónsson, *J. Phys. Chem. B* **2004**, *108*, 17886–17892.

[4] a) T. Jacob, R. P. Muller, W. A. Goddard, *J. Phys. Chem. B* **2003**, *107*, 9465–9476; b) T. Jacob, W. A. Goddard III, *ChemPhysChem* **2006**, *7*, 992–1005; c) T. Jacob, *Fuel Cells* **2006**, *6*, 159–181; d) J. A. Keith, G. Jerkiewicz, T. Jacob, *ChemPhysChem* **2010**, *11*, 2779–2794.

[5] *Jaguar*, Schrödinger, LLC, New York, NY, **2007**.

[6] a) J. L. Gland, B. A. Sexton, G. B. Fisher, *Surf. Sci.* **1980**, *95*, 587–602; b) C. Campbell, G. Ertl, H. Kuipers, J. Segner, *Surf. Sci.* **1981**, *107*, 220–236; c) D. H. Parker, M. E. Bartram, B. E. Koel, *Surf. Sci.* **1989**, *217*, 489–510.

[7] a) S. Lehwald, H. Ibach, H. Steininger, *Surf. Sci.* **1982**, *117*, 342–351; b) H. Steininger, S. Lehwald, H. Ibach, *Surf. Sci.* **1982**, *123*, 1–17; c) P. D. Nolan, B. R. Lutz, P. L. Tanaka, J. E. Davis, C. B. Mullins, *J. Chem. Phys.* **1999**, *111*, 3696–3704.

[8] G. B. Fisher, J. L. Gland, *Surf. Sci.* **1980**, *94*, 446–455.

[9] B. C. Stipe, M. A. Rezaei, W. Ho, S. Gao, M. Persson, B. I. Lundqvist, *Phys. Rev. Lett.* **1997**, *78*, 4410–4413.

[10] a) A. Damjanovic, V. Brusic, *Electrochim. Acta* **1967**, *12*, 615–628; b) D. Sepa, M. Vojnovic, L. Vracar, A. Damjanovic, *Electrochim. Acta* **1987**, *32*, 129–134.

[11] a) S. J. Clouser, J. C. Huang, E. Yeager, *J. Appl. Electrochem.* **1993**, *23*, 597–605; b) E. Yeager, M. Razaq, D. Gervasio, A. Razaq, D. Tryk, *J. Serb. Chem. Soc.* **1992**, *57*, 819–833.

[12] B. Grgur, N. Marković, P. Ross, *Can. J. Chem.* **1997**, *75*, 1465–1471.

[13] L. Qi, X. Qian, J. Li, *Phys. Rev. Lett.* **2008**, *101*, 146101.

[14] J. O. Bockris, A. K. Reddy in *Modern Electrochemistry 2B: Electrodics in Chemistry, Engineering, Biology and Environmental Science* Kluwer Academic/Plenum Publishers, New York, **2001**, pp. 1539–1550.

[15] N. Markovic, R. Adzic, B. Cahan, E. Yeager, *J. Electroanal. Chem.* **1994**, *377*, 249–259.

[16] H. Eyring, *J. Chem. Phys.* **1935**, *3*, 107–115.

[17] D. Marx, *ChemPhysChem* **2006**, *7*, 1848–1870.

[18] N. M. Markovic, H. A. Gasteiger, P. N. Ross, *J. Phys. Chem.* **1995**, *99*, 3411–3415.

